

# Thermodynamic Comparison of the Interactions of Cholesterol with Unsaturated Phospholipid and Sphingomyelins

Alekos Tsamaloukas, Halina Szadkowska, and Heiko Heerklotz

Department of Biophysical Chemistry, Biocenter of the University of Basel, Basel, Switzerland

**ABSTRACT** A comparative analysis of the interaction of cholesterol (Chol) with palmitoyl-oleoyl-phosphatidylcholine (POPC) and sphingomyelins (SM) was performed in largely homogeneous, fluid-phase membranes at 50°C. To this end, three independent assays for isothermal titration calorimetry were applied to POPC/SM/Chol mixtures. Cholesterol is solubilized by randomly methylated- $\beta$ -cyclodextrin and the uptake of Chol into (or release from) large unilamellar vesicles is measured. The affinity of Chol to a POPC/SM (1:1) membrane with 30 mol % Chol is approximately two times higher than to POPC alone; extrapolation to pure SM yields an affinity ratio of  $R_K \sim 5$ . Bringing Chol in contact with SM is highly exothermic (–7 kJ/mol for POPC/SM (1:1), and –13 kJ/mol extrapolated to pure SM, both compared to POPC). No pronounced differences were observed between egg, bovine brain, and palmitoyl SM. With decreasing Chol content,  $R_K$  increases and  $\Delta H$  becomes more exothermic, suggesting a trend toward superlattice formation. That SM/Chol-interactions are enthalpically favorable implies that the preference of Chol for SM increases upon cooling and can induce domain formation below a certain temperature. The enthalpy gain is partially compensated by a loss in entropy in accordance with the concept of Chol-induced chain ordering, which improves intermolecular interactions (van der Waals, H-bond) but reduces conformational and motional freedom. The ability of cyclodextrin to extract sphingomyelin from membranes is twofold-weaker than for POPC.

## INTRODUCTION

The organization of the plasma membrane of cells is a topic of considerable interest in contemporary membrane biology. In particular, the question whether membrane lipids form a homogenous matrix for membrane proteins to dissolve in or whether the lipids themselves show tendencies to form domains constitutes a yet-open question. Biochemical assays based on detergent treatment of cell membranes led to the concept of so-called detergent-resistant membranes (DRMs) (1)—membrane patches insoluble in cold, nonionic detergents and being enriched in cholesterol (Chol) and sphingolipids. These DRMs have been assumed to represent preexisting domains in the membrane, giving rise to the concept of so-called lipid rafts (2,3). However, in recent years both model system studies (4–7) and studies with biological specimens (8–9,10) have put the “DRM = raft” hypothesis into question (for reviews see, e.g., (11–14)) so that insight into detergent-free membranes is urgently needed.

Cholesterol, among its diverse functions in biological membranes, is believed to be of considerable importance for the formation of domains. Preferential interactions of Chol with different lipids could account for the uneven distribution among intracellular membranes (15) and cholesterol-induced domain formation. To quantify these, various experimental assays have been described in the literature. For example, Lange et al. (16) studied the exchange of Chol between erythrocyte ghost membranes and phospholipid vesicles whereas Yeagle and Young (17) monitored Chol

exchange between vesicles of different size. To overcome the problem caused by slow equilibration processes observed in these types of experiments, only recently the use of cyclodextrins (Cyds) was established (18–22). Niu and Litman (23) measured differential affinities of Chol for different lipids using binary Cyd-lipid vesicle systems. In relating partition coefficients of Chol between Cyd and differently composed lipid vesicles, they were able (by employing a thermodynamic cycle) to quantify differential affinities of Chol for different lipids.

Following a similar rationale, we have recently established two convenient assays for isothermal titration calorimetry (ITC) (24), measuring either the uptake of or the release of Chol by lipid vesicles. One important advantage of the calorimetric approach is that not only affinities but also enthalpic and entropic contributions to the partitioning process can be quantified (25). Unfortunately, it was impossible to apply the techniques introduced for palmitoyl-oleoyl-phosphatidylcholine (POPC) simply to vesicles of sphingomyelin (SM) since their equilibration kinetics are much too slow. We have resolved this problem by two strategies. First, we have studied the effect of varying amounts of SM added to POPC vesicles. Second, we have developed an alternative assay similar to the partitioning protocol of Zhang and Rowe (26). These authors studied the interaction of *n*-butanol with various phases of dipalmitoylphosphatidylcholine. Their protocol is based on a null-experiment injecting lipid-alcohol mixed vesicles into solutions of different alcohol concentration. They searched for the situation where the observable heat effects change from endothermic to exothermic with the point of vanishing heat signal yielding the partition coefficient (free alcohol concentration in the syringe matches the

Submitted December 27, 2005, and accepted for publication March 3, 2006.

Address reprint requests to H. Heerklotz, Tel.: 41-61-267-2180; E-mail: heerklotz@gmx.net.

© 2006 by the Biophysical Society

0006-3495/06/06/4479/09 \$2.00

doi: 10.1529/biophysj.105.080127

one present in the calorimeter cell). Similar reasoning can be applied to the partitioning of Chol and will be illustrated herein for the first time.

We apply the three aforementioned assays to study the interaction of Chol with lipid mixtures composed of 1-palmitoyl-2-oleoyl-*sn*-glycero-3-phosphocholine (POPC) and sphingomyelin (SM) of different origin. A major issue for these experiments is the fact that sphingomyelins have high chain melting temperatures ranging between  $T_m \sim 37$  and  $53^\circ\text{C}$  (27–29) and that gel phase membranes are rather poor acceptors of cholesterol (17). To avoid misleading conclusions arising from nonhomogeneous membranes and also in line with other experimental studies like fluorescence (30,31), NMR (32,33), ESR (34), and x-ray diffraction (28,35) working (partially) at elevated temperatures, we have conducted our partitioning experiments at  $T = 50^\circ\text{C}$ . Taking this precaution, we seek to minimize the effect that a domain-containing membrane has on the thermodynamic parameters accessible by ITC, i.e., the partition coefficient ( $K_X$ ) and enthalpy ( $\Delta H$ ). On the basis of these results, we also discuss the behavior expected at lower temperature.

## THEORY

The partitioning process of cholesterol from Cyd/Chol complexes into a membrane (or the release from a membrane into Cyd/Chol complexes) can be analyzed within the framework of our recently established model (24). Briefly, a Cyd/membrane partition coefficient may be defined via

$$K_X = \frac{c_{\text{Chol}}^b c_{\text{Cyd}}^2}{(c_L + c_{\text{Chol}}^b) c_{\text{Cyd}}}, \quad (1)$$

where  $c_{\text{Chol}}^b$  denotes the concentration of membrane-bound and  $c_{\text{Chol}}^{\text{Cyd}}$  the concentration of Cyd-complexed cholesterol,  $c_L$  stands for the lipid concentration, and  $c_{\text{Cyd}}$  for the concentration of free cyclodextrin. The term  $c_{\text{Cyd}}$  is squared since the predominant Chol/Cyd-binding stoichiometry was shown to be 1:2 (24). Upon inserting  $c_{\text{Chol}}^{\text{Cyd}} = c_{\text{Chol}} - c_{\text{Chol}}^b$  (where  $c_{\text{Chol}}$  is the total Chol concentration) into Eq. 1, a second-order polynomial in  $c_{\text{Chol}}^b$  results, with the physically meaningful solution given by

$$c_{\text{Chol}}^b = \frac{c_L - c_{\text{Chol}} + c_{\text{Cyd}}^2/K_X}{2}, \quad \left[ \sqrt{1 + 4 \frac{c_L c_{\text{Chol}}}{(c_L - c_{\text{Chol}} + c_{\text{Cyd}}^2/K_X)}} - 1 \right]. \quad (2)$$

## MATERIALS AND METHODS

### Substances and sample preparation

The lipids 1-palmitoyl-2-oleoyl-*sn*-glycero-3-phosphocholine (POPC), egg (eSM), and bovine brain (bSM) sphingomyelin were purchased from Avanti

Polar Lipids (Alabaster, AL). *N*-Palmitoyl-sphingomyelin (pSM) was a kind gift of Peter J. Slotte (Åbo Akademi University, Turku, Finland). Cholesterol (Chol) and randomly methylated- $\beta$ -cyclodextrin (Cyd) were from Fluka (Buchs, Switzerland). Mixtures of POPC, Chol, and sphingomyelin were prepared as described (5,36). The dry lipid mixtures were suspended in 100 mM NaCl, 10 mM Tris buffer at pH 7.4 by gentle vortexing to a reach a total lipid concentration (without including the amount of Chol) of  $c_{\text{PC}} + c_{\text{SM}} = 10$  mM for the uptake and release experiments. The Rowe assays (26) were performed exclusively with  $c_{\text{PC}} + c_{\text{SM}} = 15$  mM and a mole fraction of bound Chol,  $X_{\text{Chol}} = 0.2$ . Large unilamellar vesicles (LUVs) were prepared by 10 extrusion runs through a Nucleopore polycarbonate filter at  $50^\circ\text{C}$  in a Lipex extruder (Northern Lipids, Vancouver, Canada).

## ITC measurements

All ITC experiments were performed at  $T = 50^\circ\text{C}$  on a VP ITC calorimeter from MicroCal (Northampton, MA) (37,38) as described in detail elsewhere (24). Briefly, in the case of the release assay, mixed POPC/SM LUVs with a well-defined amount of membrane-bound Chol,  $X_{\text{Chol}} = 0.2$  or  $X_{\text{Chol}} = 0.3$ , were titrated into a solution with  $c_{\text{Cyd}} = 5$  mM and the release of Chol from the membrane into Cyd/Chol complexes was measured. For the uptake assay, Chol-free LUVs were titrated into Cyd solutions of  $c_{\text{Cyd}} = 5$  mM including varying amounts of Chol,  $c_{\text{Chol}} = 0$ –110  $\mu\text{M}$ . Blank experiments injecting lipid vesicles into Cyd (uptake) and lipid/Chol vesicles into buffer (release) yielded, as shown previously for POPC (24), small heats ( $\sim 0.2$  kJ/mol) arising from the dilution of the vesicles, lipid/Cyd interactions, imperfect temperature adjustment of the titrant, and other effects not related to Chol partitioning. The blank heats are assumed to cover most (but not all) heat effects that are not considered in our model and were, therefore, subtracted from the Chol uptake and release data before fitting. Data are displayed as normalized heats,  $Q_{\text{obs}}$ , with normalization to the amount of lipidic material (excluding Chol) injected.

To overcome the issue of very slow partitioning kinetics, we have additionally applied a strategy similar to the Rowe protocol (26) for samples with large mol fractions of SM. This protocol works as follows: Lipid vesicles with a fixed amount of membrane-bound Chol,  $X_{\text{Chol}}$  (in our case, only mixed POPC/eSM vesicles with  $X_{\text{Chol}} = 0.2$  were studied utilizing this assay), are loaded into the injection syringe and the heat resulting from injecting an aliquot of 10  $\mu\text{L}$  into the calorimeter cell was measured. The cell was filled with solutions of fixed Cyd concentration,  $c_{\text{Cyd}} = 5$  mM, but variable Chol concentration,  $c_{\text{Chol}}^{\text{cell}} = 0$ –100  $\mu\text{M}$ . The heat,  $DH$  (given in  $\mu\text{cal}$ ), obtained from each experiment conducted at different  $c_{\text{Chol}}^{\text{cell}}$ , was corrected by the value obtained in a blank experiment, i.e., titration of the same vesicles into buffer. From a plot of the corrected  $DH$ -values as a function of  $c_{\text{Chol}}^{\text{cell}}$ , both the partition coefficient and enthalpy can be obtained (see below). Even if the precise determination of the titration heat is impaired severely by slow equilibration kinetics, it remains straightforward to identify the case of vanishing heat signal, i.e., the case where the  $DH(c_{\text{Chol}}^{\text{cell}})$ -curve intercepts with the  $c_{\text{Chol}}^{\text{cell}}$  axis. Thus, a determination of the partition coefficient was always possible, whereas the enthalpy for partitioning could not be determined in the case of samples with  $X_{\text{SM}} > 0.7$ .

## Data analysis

ITC uptake and release traces were modeled in a Microsoft Excel spreadsheet according to the equation (see (24) for further details)

$$Q_{\text{obs}}(c_L) = \frac{\Delta c_{\text{Chol}}^b}{\Delta c_L} \Delta H + Q_{\text{dil}}, \quad (3)$$

with the molar enthalpy of transfer  $\Delta H$  (always given for uptake of Chol by the membrane). Since a blank subtraction (see above) can never eliminate unwanted heat effects perfectly, we have additionally allowed for an adjustable constant referred to as  $Q_{\text{dil}}$  in Eq. 3.

In case of the Rowe assay, the heat consumed (or released) upon the first 10  $\mu\text{L}$  injection (denoted by  $\Delta V_2$ ),  $\Delta H$ , is plotted as a function of the Chol concentration loaded into the cell,  $c_{\text{Chol}}^{\text{cell}}$ . The first injection of 1  $\mu\text{L}$  is not considered for the data evaluation, because it is subject to larger errors (39). However, the material injected into (or replaced from) the cell by this injection has to be considered for a correct determination of  $K_X$  and  $\Delta H$ , respectively. From the intercept with the  $c_{\text{Chol}}^{\text{cell},0}$ -axis,  $c_{\text{Chol}}^{\text{cell},0}$ , the partition coefficient  $K_X$  can be calculated using Eq. 1 and equating  $c_{\text{Chol}}^{\text{cell},0} = c_{\text{Chol}}^{\text{Cyd}}$ . Here both parameters, i.e.,  $K_X$  and  $\Delta H$ , were obtained by fitting the following relation (used in an Excel spreadsheet) to the experimental data,

$$\begin{aligned} \Delta H &= \Delta c_{\text{Chol}}^b \Delta H V_0 \\ &= \left\{ c_{\text{Chol}}^b(2) \left( 1 + \frac{\Delta V_2}{2V_0} \right) + c_{\text{Chol}}^b(1) \left( \frac{\Delta V_2}{2V_0} - 1 \right) \right. \\ &\quad \left. - \frac{\Delta V_2}{V_0} c_{\text{Chol}}^{\text{syrr}} \right\} \Delta H V_0, \end{aligned} \quad (4)$$

where  $\Delta c_{\text{Chol}}^b$  stands for the change in concentration of membrane-bound Chol occurring upon the second injection,  $V_0$  is the cell volume of 1.4 mL, and  $c_{\text{Chol}}^{\text{syrr}}$  is the bound (= total) Chol concentration present in the injection syringe. The expressions  $c_{\text{Chol}}^b(i)$  are calculated on the basis of Eq. 2 using corrected concentrations as explained in Tsamaloukas et al. (24).

Generally,  $K_X$  and  $\Delta H$  values obtained in the modeling of the data are listed with estimated maximal errors of  $\delta(K_X) = 20\%$ , and  $\Delta(\Delta H) = \pm 2$  kJ/mol for  $c_{\text{SM}}/(c_{\text{SM}} + c_{\text{PC}}) < 0.5$ , and  $\delta(K_X) = 40\%$  and  $\Delta(\Delta H) = \pm 4$  kJ/mol above this ratio, respectively.

## RESULTS

### Uptake and release assay

Fig. 1 shows representative experimental raw data as well as the global analysis of Chol uptake and release data. For the release experiment, 10 mM LUVs with mol fractions of pSM,  $X_{\text{pSM}} = 0.25$ , and Chol,  $X_{\text{Chol}} = 0.2$  were titrated into a solution with  $c_{\text{Cyd}} = 5$  mM. In case of the uptake experiment, 10 mM LUVs with  $X_{\text{pSM}} = 0.25$  were titrated into a solution with  $c_{\text{Cyd}} = 5$  mM, and  $c_{\text{Chol}} = 70$   $\mu\text{M}$ ,

respectively. For both experiments conducted at 50°C the injection protocol consisted of  $1 \times 1$   $\mu\text{L}$ ,  $3 \times 5$   $\mu\text{L}$ , and  $26 \times 10$   $\mu\text{L}$  injections to better resolve the steep part of the curve at the beginning.

Independent analysis of the uptake trace yields for the model parameters entering into Eq. 3:  $K_X = 101$  mM,  $\Delta H = -10$  kJ/mol, and  $Q_{\text{dil}}^{\text{up}} = -0.001$  kJ/mol. The release data set is best modeled with  $K_X = 72$  mM,  $\Delta H = -13$  kJ/mol, and  $Q_{\text{dil}}^{\text{rel}} = -0.1$  kJ/mol, while the global fit results in  $K_X = (79 \pm 16)$  mM,  $\Delta H = -(13 \pm 2)$  kJ/mol,  $Q_{\text{dil}}^{\text{up}} = 0.1$  kJ/mol, and  $Q_{\text{dil}}^{\text{rel}} = -0.1$  kJ/mol, respectively.

### Rowe assay

As pointed out already, uptake/release partitioning assays become impractical due to extremely slow reequilibration after an injection for vesicles containing large amounts of SM. A solution to this problem is a modified Rowe assay (26). Fig. 2 shows raw experimental data as well as the modeling of the data according to Eq. 4. LUVs composed of 50 mol % eSM, 20 mol % Chol, and 30 mol % POPC at a total lipid concentration,  $c_{\text{PC}} + c_{\text{SM}} = 15$  mM, were titrated into Cyd solutions ( $c_{\text{Cyd}} = 5$  mM) including different concentrations of Chol,  $c_{\text{Chol}}^{\text{cell}} = 0$ –60  $\mu\text{M}$ . Analysis of the data shown in Fig. 2B according to Eq. 4 yields  $K_X = (147 \pm 59)$  mM and  $\Delta H = -(20 \pm 4)$  kJ/mol, respectively.

### Summary of the Chol partitioning experiments

An overview of the experimental results obtained with both uptake/release assay and Rowe assay is provided with Fig. 3. Displayed are the partition coefficient,  $K_X$ , and molar enthalpy change,  $\Delta H$ , as a function of membrane composition given as the mole fraction of SM among the phospholipids:

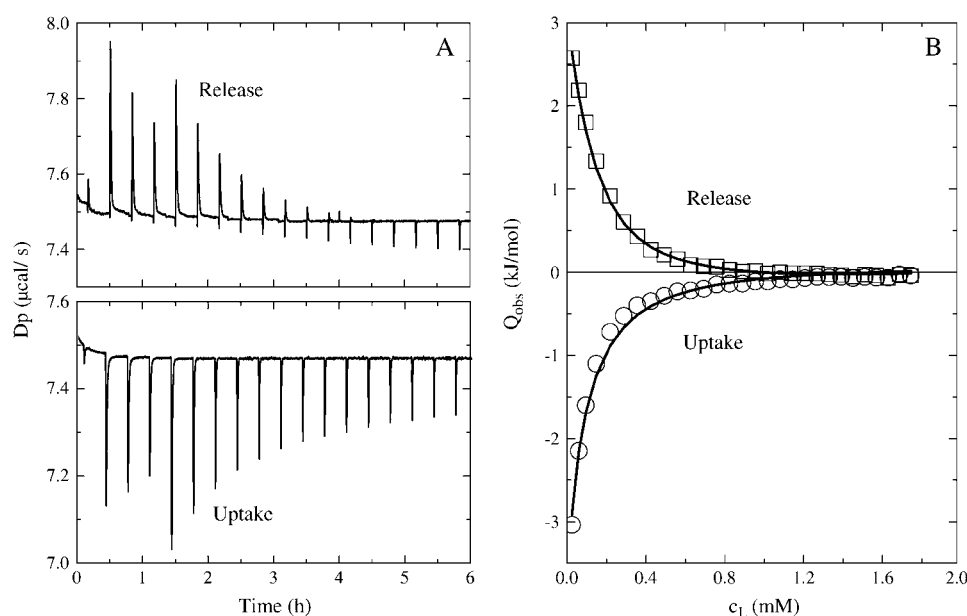


FIGURE 1 Experimental raw data of Chol uptake and release assay conducted at 50°C. For the release assay, 10 mM lipid vesicles with a mol fraction of pSM,  $X_{\text{pSM}} = 0.25$ , and a mol fraction of Chol,  $X_{\text{Chol}} = 0.2$ , were titrated into a 5 mM Cyd solution. In case of the uptake assay, vesicles with  $X_{\text{pSM}} = 0.25$  without Chol were titrated into a 5 mM Cyd + 70  $\mu\text{M}$  Chol solution. For both raw data sets shown in panel A, the injection protocol was  $1 \times 1$   $\mu\text{L}$ ,  $3 \times 5$   $\mu\text{L}$ , and  $26 \times 10$   $\mu\text{L}$ . (B) Global fit (solid lines) to the normalized heats,  $Q_{\text{obs}}$ , of uptake (○) and release (□) assay resulting after integration of the power peaks shown in panel A. Data are corrected for the heats obtained in blank experiments (see section on ITC experiments).

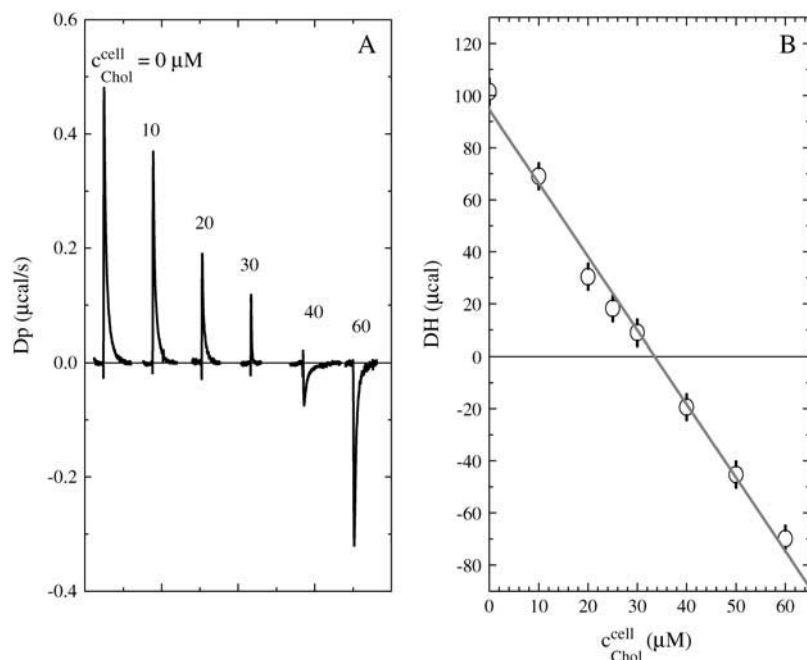


FIGURE 2 (A) Detail of the experimental raw data obtained with the Rowe protocol at 50°C. An aliquot of  $\Delta V_2 = 10 \mu\text{L}$  of vesicles with  $X_{\text{eSM}} = 0.5$ ,  $X_{\text{Chol}} = 0.2$ , and  $X_{\text{PC}} = 0.3$  was injected into a 5 mM Cyd-solution with varying Chol concentration,  $c_{\text{Chol}}^{\text{cell}}$ , as depicted in the plot. (B) Heats  $DH$  resulting from an integration of the power peaks shown in panel A (after blank correction) as a function of  $c_{\text{Chol}}^{\text{cell}}$ . The partition coefficient  $K_X$  can be calculated from the intercept with the  $c_{\text{Chol}}^{\text{cell}}$  axis and the molar transfer enthalpy,  $\Delta H$ , can be obtained using Eq. 4.

$x \equiv c_{\text{SM}}/(c_{\text{SM}} + c_{\text{PC}})$  (excluding the variable Chol concentration, merely for practical reasons). The origin ( $x = 0$ ) corresponds to the case of Chol partitioning into a POPC membrane (with the respective values taken from (24)) and the point  $x = 1$  accordingly to the partitioning into a SM membrane. Solid symbols represent results for eSM with  $X_{\text{Chol}} = 0.3$ , which were obtained by global fits (*solid circles*) and, at high SM content, individual uptake curves (*solid triangle*). The partition coefficient,  $K_X$ , increases with increasing amount of SM in the vesicles, and the partitioning enthalpy,  $\Delta H$ , becomes increasingly exothermic. In general, the latter shown in Fig. 3 B was included only up to mixtures with  $x < 0.9$ , as its assignment (independently of the assay used) above this value was not considered to be reliable (see also below). Release experiments were impossible to be performed above  $x = 0.8$ . As such, the error bars given for these points are significantly larger (see Materials and Methods) than those given for values obtained in global analysis of uptake/release data sets at small  $c_{\text{SM}}$ .

We have evaluated  $K_X(x)$  and  $\Delta H(x)$  according to a model based on pairwise nonideality parameters for POPC/SM, POPC/Chol, and, SM/Chol, analogously to the procedure described in (40) (data not shown). The resulting fits were virtually linear but a precise determination of the nonideality parameters is impossible without accurate additional information. Therefore, we excluded the model here and refer to quasi-empirical, linear fits of the data (*solid and dashed lines* in Fig. 3). Results for  $K_X$  and  $\Delta H$  at  $x = 0$  (taken from (24)),  $x = 0.5$ , and linearly extrapolated to  $x = 1$  are given in Table 1. Open symbols (*diamond, down-triangle, and circle*) in Fig. 3 specify parameters obtained with eSM vesicles incorporating 20 mol % Chol. Results obtained by global data analysis of

uptake/release assay with pSM vesicles,  $X_{\text{Chol}} = 0.2$ , are depicted by the cross-hair symbols in Fig. 3. Generally, up to  $x = 0.5$ , no pronounced deviation from the behavior of eSM vesicles is observed. A spot-check experiment (uptake assay) with bSM vesicles,  $X_{\text{Chol}} \sim 0.3$ , is similarly described by parameters that agree within error with those collected for the other sphingomyelins used in this study (see the *plus symbol* in Fig. 3).

In summary, we find no significant deviations between the results of different assays (uptake, release, Rowe) and between different sphingomyelins (eSM, pSM, bSM). For both  $K_X$  and  $\Delta H$ , a larger scatter appears for  $x > 0.5$ . Differential scanning calorimetry experiments (data not shown), suggest that for samples with  $X_{\text{SM}} > 0.5$  and  $X_{\text{Chol}} = 0.2$  or 0.3, the main transition of the lipids is not fully completed at 50°C. Therefore, the deviations we observe may be due to residual gel phase domains in an otherwise already fluid phase membrane.

### Lipid extraction assay

Employing the protocol established by Anderson et al. (41), the dissolution of pure eSM vesicles by Cyd at 50°C was measured as shown in Fig. 4. LUVs with  $c_L = 5, 8$ , and 10 mM were titrated in 5  $\mu\text{L}$  aliquots into the calorimeter cell containing Cyd solutions with  $c_{\text{Cyd}} = 20\text{--}60$  mM. In the beginning of the titration, all injected vesicles are dissolved by the Cyd, giving rise to constant heat signals. When a characteristic mole ratio of lipid per Cyd is reached in the calorimeter cell, the heats of titration change (breakpoints indicated by *arrows* in Fig. 4), indicating a saturation of the Cyd by the injected lipid. Knowledge of these breakpoints can be used to estimate the lipid/Cyd association constant,

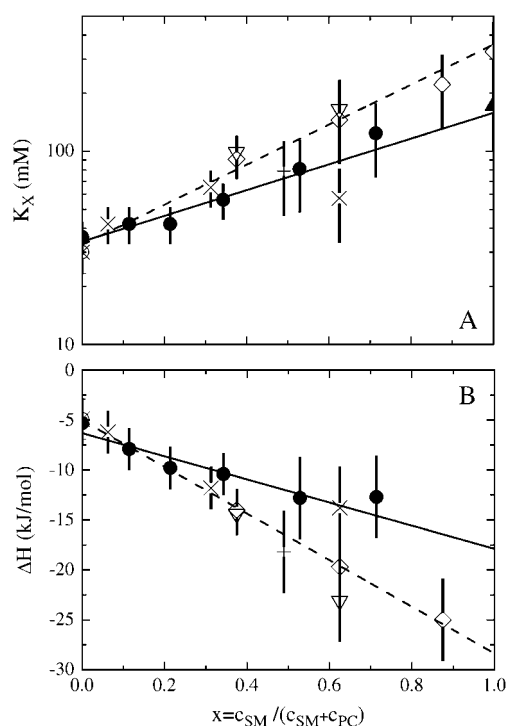


FIGURE 3 The cyclodextrin-membrane partition coefficient,  $K_X$  (A), and the molar transfer enthalpy,  $\Delta H$  (B), of cholesterol measured for various POPC/SM mixtures at  $T = 50^\circ\text{C}$ . For both panels symbols used correspond to global analysis of ITC uptake/release data sets of POPC/eSM vesicles with  $X_{\text{Chol}} \sim 0.3$  (●), POPC/pSM vesicles with  $X_{\text{Chol}} \sim 0.2$  (×), Rowe protocol for POPC/eSM vesicles with  $X_{\text{Chol}} = 0.2$  (◇), uptake experiments with POPC/eSM (▲) and POPC/bSM vesicles (+), and release experiment (▽) with POPC/eSM vesicles with  $X_{\text{Chol}} = 0.2$ . Solid lines in both panels correspond to linear fits to the POPC/eSM data with  $X_{\text{Chol}} = 0.3$  (●), and dashed lines to POPC/eSM data with  $X_{\text{Chol}} = 0.2$  (◇). For both data sets, the point at  $x = c_{\text{SM}}/(c_{\text{SM}} + c_{\text{PC}}) = 0$  was taken from Tsamaloukas et al. (24).

$K_\Phi$ , using Eq. 5, which is based on a thermodynamic coexistence of membranes and lipid-saturated Cyd (41). Assuming that the inclusion complex has the same stoichiometry as shown for POPC in Anderson et al. (41), i.e., one lipid per four cyclodextrins, we can calculate  $K_\Phi$  via

$$K_\Phi = \frac{1}{c_{\text{Cyd}}^3} \frac{R_{\text{SM/Cyd}}}{(1 - 4R_{\text{SM/Cyd}})^4}, \quad (5)$$

where  $R_{\text{SM/Cyd}}$  is the molar ratio of SM and Cyd in the calorimeter cell at the position of the breakpoint. We obtain as mean value from the traces shown in Fig. 4:  $K_\Phi(\text{eSM}) = (295 \pm 60) (\text{M})^{-3}$ . This value is smaller than the one for POPC resulting by interpolation of the data given in Anderson et al. (41) to  $50^\circ\text{C}$ :  $K_\Phi(\text{POPC}) = (531 \pm 106) (\text{M})^{-3}$ . Data shown in Fig. 4B are normalized with respect to the amount of lipid injected but not blank-corrected. The appropriate blank titrations as utilized in Anderson et al. (41), i.e., injection of buffer into Cyd solutions at the respective concentrations yield constant heat values (data not shown), indicating that heats of dilution have no effect on the position of the breakpoint.

## DISCUSSION

### PC→SM transfer of Chol

Analogously to the thermodynamic cycle used by Niu and Litman (23), we can discuss differences between Chol interactions with membranes of different SM content,  $x$ , independently of cyclodextrin, by comparing different points on the linear regressions to the  $K_X(x)$  and  $\Delta H(x)$  data shown in Fig. 3. The ratio  $R_K \equiv K_X(x)/K_X(0)$  is, again, a partition coefficient: that for Chol between SM-containing membranes and pure POPC membranes. Similarly, the enthalpy difference  $\Delta(\Delta H) \equiv \Delta H(x) - \Delta H(0)$  corresponds to the enthalpy of transfer of Chol from a POPC membrane into a SM-containing membrane. The values of  $R_K$  given in Table 1 imply that Chol would accumulate to an  $\sim 5$ – $12$ -fold concentration in a hypothetical pure SM domain coexisting with a pure PC domain. The transfer to SM would yield an enthalpy gain of  $\Delta(\Delta H) \sim -(13\text{--}23) \text{ kJ/mol}$ . Equivalently, intermolecular interactions of Chol would contribute favorably by  $\Delta(\Delta\mu^0) \sim -5 \text{ kJ/mol}$  ( $X_{\text{Chol}} = 0.3$ , see Table 1) to the standard free energy change of demixing of a membrane into POPC and SM domains. Demixing is, of course, opposed by

TABLE 1 Results obtained with the data fitting in Fig. 3 and derived quantities

Membrane	$X_{\text{Chol}}$ (%)	$K_X$ (mM)	$R_K(50^\circ\text{C})$	$R_K(37^\circ\text{C})$	$\Delta(\Delta\mu^0)$	$\Delta H$	$\Delta(\Delta H)$	$-T\Delta(\Delta S^0)$
					kJ/mol			
PC	20	30	1.0	1.0	0	−5	0	0
PC/SM (1:1)	20	108	3.6	4.3	−4	−17	−12	8
SM	20	360	12	17	−8	−28	−23	15
PC	30	35	1.0	1.0	0	−5	0	0
PC/SM (1:1)	30	73	2.1	2.3	−2	−12	−7	5
SM	30	158	4.5	5.5	−5	−18	−13	8

$K_X$  denotes the cyclodextrin/membrane partition coefficient,  $R_K$  is the ratio between  $K_X$  for a SM-containing membrane and  $K_X$  for pure POPC as determined in Tsamaloukas et al. (24). The value  $\Delta(\Delta\mu^0)$  is the standard chemical potential difference of Chol insertion (compared to POPC),  $\Delta(\Delta\mu^0) = -RT \ln(R_K(50^\circ\text{C}))$ ,  $\Delta H$  is the enthalpy of transfer of Chol from Cyd into the membrane, and  $\Delta(\Delta H)$  is the enthalpy of Chol transfer from POPC into the membrane of interest assumed to be equal to the enthalpy change under standard conditions,  $\Delta(\Delta H^0)$ . The standard entropy change of Chol transfer from POPC into another membrane is obtained as  $-T\Delta S^0 = \Delta(\Delta\mu^0) - \Delta(\Delta H)$ . Values of  $R_K(37^\circ\text{C})$  were estimated from  $R_K(50^\circ\text{C})$  and  $\Delta(\Delta H)$  using a modified van't Hoff equation:  $d(\ln(R_K)) = dT \Delta(\Delta H)/(RT^2)$ , assuming  $\Delta(\Delta H)$  to be constant. Errors for the parameters are as detailed under Materials and Methods.

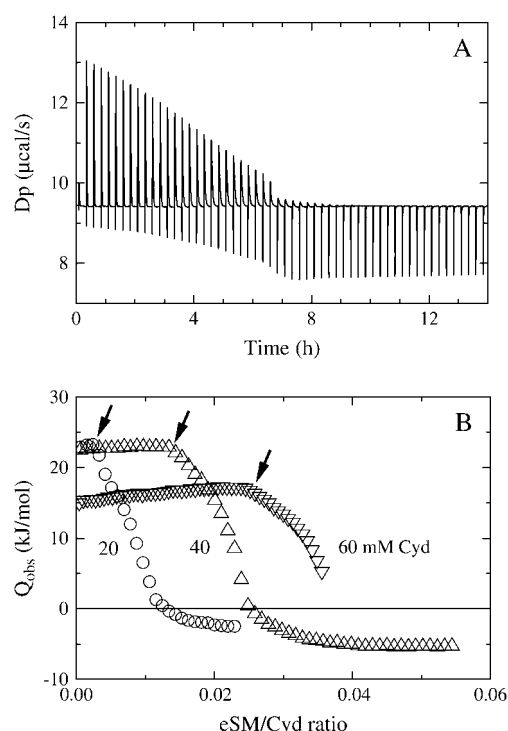


FIGURE 4 Titration of eSM vesicles into Cyd solutions at  $T = 50^\circ\text{C}$ . (A) Titration of 8 mM eSM LUVs into a 40 mM Cyd solution using  $1 \times 1\mu\text{L}$  (see text) and  $56 \times 5\mu\text{L}$  aliquots. (B) Normalized heats,  $Q_{\text{obs}}$ , resulting after integration of the power peaks shown in panel A for titrations of a 20 mM Cyd ( $\circ$ ), 40 mM Cyd ( $\Delta$ ), and 60 mM Cyd solution ( $\nabla$ ) with 5, 8, and 10 mM eSM LUVs, respectively. Data shown in panel B are not corrected for the heats obtained in titrations of the respective Cyd solutions with buffer (see text). Arrows indicate the solubilization boundary for each titration curve.

the entropy of mixing and would therefore, if it occurs at all, not lead to pure POPC and SM but only to POPC-rich and SM-rich domains.

### The effect of the Chol concentration

Comparing the data at  $X_{\text{Chol}} = 0.3$  (solid symbols) with those at smaller Chol concentration,  $X_{\text{Chol}} = 0.2$  (open symbols), we find a significant increase in  $K_X$  and  $R_K$  and more exothermic enthalpy changes,  $\Delta H$  and  $\Delta(\Delta H)$ , at the lower cholesterol content (see Table 1). It is intriguing that  $X_{\text{Chol}}$  has opposite effects on  $K_X$  and  $\Delta H$  of POPC and SM, as indicated by the solid and dashed lines in Fig. 3 crossing each other. Whereas  $K_X$  of POPC increases slightly with increasing cholesterol content (24), it decreases markedly for SM. This has important implications for the mixing behavior of SM/Chol membranes, since it causes a tendency to avoid Chol/Chol contacts and to arrange molecules in a nonrandom fashion to increase the number of mixed, SM/Chol contacts. Such behavior is the basis for the formation of superlattices, which have indeed been found for SM/Chol systems under certain conditions (42,43). An explanation for such a behavior was given in terms of the umbrella model (44).

### Thermodynamics of SM/Chol interactions

The knowledge of  $\Delta H$  also yields the entropic contribution to SM/Chol compared to POPC/Chol interactions. Since the enthalpy of Chol transfer from POPC to SM measured here,  $\Delta(\Delta H)$ , should approximately agree with the enthalpy under standard conditions,  $\Delta(\Delta H^0)$ , we may apply  $\Delta(\Delta\mu^0) = \Delta(\Delta H^0) - T\Delta(\Delta S^0)$  to derive the entropic contribution to SM/Chol interactions. We find that SM/Chol interactions are accompanied by a strong, unfavorable loss in entropy that is contributing  $-T\Delta(\Delta S^0) \sim +(8-15)$  kJ/mol to the standard free energy (Table 1). This behavior is in accord with the concept of Chol-induced ordering of SM chains. This improves molecular packing (van der Waals interactions) and conformational enthalpy and may include formation of H-bonds ( $\Delta(\Delta H) < 0$ ), but reduces conformational and motional freedom ( $\Delta(\Delta S^0) < 0$ ). We emphasize that  $\Delta H$  per mol of Chol becoming surrounded by SM agrees with  $\sim 0.5-0.75 \times$  the enthalpy per mol of SM undergoing the fluid  $\rightarrow$  gel transition ( $\sim -30$  kJ/mol, (5,28,29)).

### Gradual changes versus domains or complexes

In general, there are two possible modes of cholesterol-induced lipid ordering: 1), gradual, unspecific ordering in a randomly mixed membrane; or 2), specific ordering of selected lipids by forming stoichiometric complexes or liquid-ordered domains (see (45) for a review). Negative  $\Delta H$  of transfer of Chol from POPC to SM could arise from both phenomena. What should differ is the dependence of  $\Delta H$  on the SM content,  $x$ , which is essentially linear for mixing but should show breakpoints at stoichiometric compositions or phase boundaries. In essentially mixed membranes, Chol/SM contacts become gradually more abundant with increasing  $x$  and a quantitative model (not shown) is compliant with a linear  $\Delta H(x)$ . If Chol forms complexes with SM, two regimes are to be expected. At SM contents below the stoichiometric composition, SM is limiting complex formation and  $|\Delta H|$  should increase with SM content,  $x$ . Above the stoichiometric SM content, SM is in excess and  $\Delta H$  (per mole of Chol) should be constant (independent of  $x$ ). A similar effect is to be expected at a phase boundary. Addition of Chol to a two-phase system should also yield a constant heat since the uptake of Chol induces a characteristic growth of the ordered phase independently of the amount of ordered phase present. For an analogous case, see constant heat of titration of detergent into a membrane-micelle equilibrium (46). The precision of our data may not warrant a strict conclusion regarding the presence of complexes or domains, but we state that we find no significant evidence for such phenomena and our results are in line with a more gradual, unspecific ordering of lipids in a largely homogeneous membrane.

We should note that the specific interaction between Chol and SM involves a considerable enthalpy and is expected to induce major structural changes to the molecules. However,

because this enthalpy is largely compensated by entropy, it does not give rise to a significant deviation of the molecules from a nonrandom arrangement. It can, therefore, not be detected by fluorescence energy transfer measurements like those performed in Holopainen et al. (47).

### Temperature dependence

Another advantage of knowing  $\Delta H$  is that it gives an estimate for the temperature dependence of the differential affinities. This is important since principal and technical problems hindered us to determine  $K_X$  at lower temperatures. Le Chatelier's principle requires that every exothermic process (such as bringing more Chol in contact with SM) is promoted by lower temperature. That means the preference of Chol for SM and its activity to induce demixing increase upon cooling so that domain formation may proceed below a certain temperature. Quantitative estimates can be obtained using a modified van't Hoff equation,  $d(\ln(R_K)) = dT \Delta(\Delta H)/(RT^2)$ . Assuming that  $\Delta(\Delta H)$  is not strongly temperature-dependent, we may estimate values for  $R_K$  at lower temperatures as given for 37°C in Table 1.

### Comparison with literature data

Let us compare these values with those given in the literature. Our calculated value of  $R_K(37^\circ\text{C}) = 5.5$  ( $X_{\text{Chol}} = 0.3$ ) for pure SM agrees with the value of 6.8 extrapolated by Niu and Litman (23) for POPC/pSM, and our prediction for POPC/eSM (1:1) is consistent with the result of Leventis and Silvius (21), who obtained  $R_K(37^\circ\text{C}) = 2.6$  for SOPC/bSM (1:1). Other authors have obtained smaller values for  $R_K$ . For instance, the data of Lange et al. (16), who monitored Chol exchange between ghost membranes and SUVs at 46°C, can be used to calculate the following values. Chol exchange between egg PC and bSM is described by a value of  $R_K = 2.0$ , and exchange between egg PC and pSM by  $R_K = 1.9$ , respectively. Yeagle and Young (17) refrained from deriving  $R_K(45^\circ\text{C})$  from similar, vesicle-vesicle transfer experiments because of too little net transfer of Chol.

A qualitatively different behavior was described recently by Veatch et al. (33), who provided detailed information on the system DOPC/DPPC/Chol. The preference of Chol for the ordered, DPPC-rich phase compared to the fluid, DOPC-rich phase is very weak, with  $R_K \sim 1.2$ –1.9. Furthermore,  $R_K$  increases from 1.2 at 20°C to 1.8 at 30°C (DOPC/DPPC, 1:2) suggesting an endothermic transfer of Chol from fluid to ordered domains with an enthalpy change of the order of +25 kJ/mol. That means that domain formation in this system is not significantly promoted by preferential interactions of Chol with the saturated lipid and that the disappearance of ordered domains at high temperature seems to be opposed by increasing preferential interactions of cholesterol. A possible explanation is that DOPC is a twofold unsaturated lipid so that its structural preferences differ more from DPPC than

those for POPC from SM (see also (7,48) for a discussion of the behavior of monounsaturated versus polyunsaturated lipid species). Hence, demixing in the DOPC/DPPC/Chol system may be governed almost exclusively by unfavorable DOPC/DPPC interactions, whereas that in POPC/SM is substantially promoted by Chol.

### Lipid versus Chol extraction

An important issue for the application of Cyd to manipulate the Chol content of both model and cell membrane systems (20,49) is the question of which Cyd concentrations are allowed to be used in order to leave the membrane intact. We have investigated the extraction of fluid phase SM by Cyd as shown in Fig. 4, utilizing the protocol established by Anderson et al. (41). Based on the values obtained for the complex formation constant,  $K_\Phi$ , it appears that at least at 50°C, the affinity of SM for the inclusion complex with Cyd is approximately half as large as that of POPC. This observation reflects that either Cyd/SM interactions are less favorable than Cyd/POPC interactions or that SM/SM interactions within the membrane are more attractive than PC/PC interactions. The latter is in line with the respective hydrogen-bonding properties (50).

In a previous study (24), we have shown that even for a POPC membrane, the Cyd concentration window where Chol is selectively extracted without also removing phospholipid and thus solubilizing the membrane as such, is rather narrow. For example, a Cyd concentration of 15 mM added to a POPC/Chol vesicle suspension of 0.7 mM POPC and 0.3 mM Chol, extracts ~10% of the POPC, but 90% of the Chol (calculated for  $T = 50^\circ\text{C}$ ). The data collected here imply that the problem is even more serious in the presence of SM. Although SM itself is less extracted than POPC, the presence of SM opposes the extraction of Chol due to favorable SM/Chol interactions in the membrane. In our example (15 mM Cyd, 0.7 mM phospholipid, 0.3 mM Chol), 90% of Chol would be extracted from a POPC membrane but only 75% from a POPC/SM (1:1) membrane. At lower temperature, extraction of Chol is suggested to be even weaker from a membrane containing SM. Apart from the simplifying assumptions made in the calculation of the retention of lipid and Chol in the membrane, we conclude that the application of Cyd to a biological membrane is not straightforward. It requires very careful monitoring of the efficacy of Chol extraction and, at the same time, the lack of extraction of other membrane constituents. Effects of Cyd application to cells might be due to the dissolution of lipid-rafts, but also a consequence of extracting other molecules or of losing other important functions of cholesterol independently of its effect on lipid domains (13).

### CONCLUSIONS

1. The affinity of Chol to eSM is ~5- to 12-fold larger compared to POPC. The preference becomes stronger with

decreasing temperature and decreasing Chol concentration.

2. There are no pronounced differences in SM/Chol interactions (affinity,  $\Delta H$ ) between egg, brain, and palmitoyl SM.
3. The transfer of Chol from POPC to SM is highly exothermic ( $\Delta(\Delta H) \sim -(13-23)$  kJ/mol) but the gain in enthalpy is largely compensated by a loss in entropy.
4. The equilibrium constant for the extraction of SM from membranes by Cyd is approximately twofold smaller than for POPC. However, the presence of SM impedes the extraction of Chol.

We thank Peter J. Slotte (Åbo Akademi University, Turku, Finland) for providing us with the pSM used in this study.

Financial support from the Swiss National Science Foundation (grant No. 31-67216.01) is gratefully acknowledged.

## REFERENCES

1. Brown, D. A., and J. K. Rose. 1992. Sorting of GPI-anchored proteins to glycolipid-enriched membrane subdomains during transport to the apical cell surface. *Cell*. 68:533-544.
2. Simons, K., and E. Ikonen. 1997. Functional rafts in cell membranes. *Nature*. 387:569-572.
3. Brown, D. A., and E. London. 2000. Structure and function of sphingolipid- and cholesterol-rich membrane rafts. *J. Biol. Chem.* 275: 17221-17224.
4. London, E., and D. A. Brown. 2000. Insolubility of lipids in TX-100: physical origin and relationship to sphingolipid/cholesterol membrane domains (rafts). *Biochim. Biophys. Acta*. 1508:182-195.
5. Heerklotz, H. 2002. Triton promotes domain formation in lipid raft mixtures. *Biophys. J.* 83:2693-2701.
6. Silvius, J. R. 2003. Role of cholesterol in lipid raft formation: lessons from lipid model systems. *Biochim. Biophys. Acta*. 1610:174-183.
7. McMullen, T. P. W., R. N. A. H. Lewis, and R. N. McElhaney. 2004. Cholesterol-phospholipid interactions, the liquid-ordered phase and lipid rafts in model and biological membranes. *Curr. Opin. Colloid Interf. Sci.* 8:459-468.
8. Melkonian, K. A., T. Chu, L. B. Tortorella, and D. A. Brown. 1995. Characterization of proteins in detergent-resistant membrane complexes from Madin-Darby canine kidney epithelial cells. *Biochemistry*. 34: 16161-16170.
9. Schuck, S., M. Honsho, K. Ekroos, A. Shevchenko, and K. Simons. 2003. Resistance of cell membranes to different detergents. *Proc. Natl. Acad. Sci. USA*. 100:5795-5800.
10. van Rhee, J., E. M. Achame, H. Janssen, J. Calafat, and K. Jalink. 2005. PIP<sub>2</sub> signaling in lipid domains: a critical reevaluation. *EMBO J.* 24:1664-1673.
11. Munro, S. 2003. Lipid rafts: elusive or illusive? *Cell*. 115:377-388.
12. Edidin, M. 2003. The state of lipid rafts: from model membranes to cells. *Annu. Rev. Biophys. Biomol. Struct.* 32:257-283.
13. Simons, K., and W. L. C. Vaz. 2004. Model systems, lipid rafts, and cell membranes. *Annu. Rev. Biophys. Biomol. Struct.* 33:269-296.
14. Lichtenberg, D., F. M. Göni, and H. Heerklotz. 2005. Detergent-resistant membranes should not be identified with membrane rafts. *Trends Biochem. Sci.* 30:430-436.
15. Wattenberg, B. W., and D. F. Silbert. 1983. Sterol partitioning among intracellular membranes. *J. Biol. Chem.* 258:2284-2289.
16. Lange, Y., J. S. D'Alessandro, and D. M. Small. 1979. The affinity of cholesterol for phosphatidylcholine and sphingomyelin. *Biochim. Biophys. Acta*. 556:388-398.
17. Yeagle, P. L., and J. E. Young. 1986. Factors contributing to the distribution of cholesterol among phospholipid vesicles. *J. Biol. Chem.* 261: 8175-8181.
18. Slotte, J. P., and S. Illman. 1996. Desorption of fatty acids from monolayers to cyclodextrins in the subphase. *Langmuir*. 12:5664-5668.
19. Yancey, P. G., W. V. Rodriguez, E. P. C. Kilsdonk, G. W. Stoudt, W. J. Johnson, M. C. Phillips, and G. H. Rothblat. 1996. Cellular cholesterol efflux mediated by cyclodextrins. *J. Biol. Chem.* 271: 16026-16034.
20. Christian, A. E., M. P. Haynes, M. C. Phillips, and G. H. Rothblat. 1997. Use of cyclodextrins for manipulating cellular cholesterol content. *J. Lipids Res.* 38:2264-2272.
21. Leventis, R., and J. R. Silvius. 2001. Use of cyclodextrins to monitor transbilayer movement and differential lipid affinities of cholesterol. *Biophys. J.* 81:2257-2267.
22. Steck, T. L., J. Ye, and Y. Lange. 2002. Probing red cell membrane cholesterol movement with cyclodextrin. *Biophys. J.* 83:2118-2125.
23. Niu, S.-L., and B. J. Litman. 2002. Determination of membrane cholesterol partition coefficient using a lipid vesicle-cyclodextrin binary system: effect of phospholipid acyl-chain unsaturation and headgroup composition. *Biophys. J.* 83:3408-3415.
24. Tsamaloukas, A., H. Szadkowska, J. P. Slotte, and H. Heerklotz. 2005. Interactions of cholesterol with lipid membranes and cyclodextrin characterized by calorimetry. *Biophys. J.* 89:1109-1119.
25. Heerklotz, H. 2004. Microcalorimetry of lipid membranes. *J. Phys. Condens. Matter*. 16:441-467.
26. Zhang, F., and E. S. Rowe. 1992. Titration calorimetric and differential scanning calorimetric studies of the interactions of *n*-butanol with several phases of dipalmitoylphosphatidylcholine. *Biochemistry*. 31: 2005-2011.
27. Barenholz, Y., J. Suurkuusk, D. Mountcastle, T. E. Thompson, and R. L. Biltonen. 1976. A calorimetric study of the thermotropic behavior of aqueous dispersions of natural and synthetic sphingomyelins. *Biochemistry*. 15:2441-2447.
28. Calhoun, W. L., and G. G. Shipley. 1979. Sphingomyelin-lecithin bilayers and their interaction with cholesterol. *Biochemistry*. 18:1717-1722.
29. Maulik, P. R., and G. G. Shipley. 1996. *N*-Palmitoyl sphingomyelin bilayers: structure and interaction with cholesterol and dipalmitoylphosphatidylcholine. *Biochemistry*. 35:8025-8034.
30. Frank, A., Y. Barenholz, D. Lichtenberg, and T. E. Thompson. 1983. Spontaneous transfer of sphingomyelin between phospholipid bilayers. *Biochemistry*. 22:5647-5651.
31. Xu, X., and E. London. 2000. The effect of sterol structure on membrane lipid domains reveals how cholesterol can induce lipid domain formation. *Biochemistry*. 39:843-849.
32. Guo, W., V. Kurze, T. Huber, N. H. Afdhal, K. Beyer, and J. Hamilton. 2002. A solid-state NMR study of phospholipid-cholesterol interactions: sphingomyelin-cholesterol binary systems. *Biophys. J.* 83: 1465-1478.
33. Veatch, S. L., I. V. Polozov, K. Gawrisch, and S. L. Keller. 2004. Liquid domains in vesicles investigated by NMR and fluorescence microscopy. *Biophys. J.* 86:2910-2922.
34. Sankaram, M. B., and T. E. Thompson. 1990. Interaction of cholesterol with various glycerolipids and sphingomyelin. *Biochemistry*. 29: 10670-10675.
35. Maulik, P. R., and G. G. Shipley. 1996. Interactions of *n*-stearoyl sphingomyelin with cholesterol and dipalmitoylphosphatidylcholine in bilayer membranes. *Biophys. J.* 70:2256-2265.
36. Heerklotz, H., H. Szadkowska, T. Anderson, and J. Seelig. 2003. The sensitivity of lipid domains to small perturbations demonstrated by the effect of Triton. *J. Mol. Biol.* 329:793-799.



37. Wiseman, T., S. Williston, J. F. Brandts, and L. N. Lin. 1989. Rapid measurement of binding constants and heats of binding using a new titration calorimeter. *Anal. Biochem.* 179:131–137.
38. Chellani, M. 1999. Isothermal titration calorimetry: biological applications. *Am. Biotechnol. Lab.* 17:14–18.
39. Heerklotz, H., and J. Seelig. 2000. Titration calorimetry of surfactant-membrane partitioning and membrane solubilization. *Biochim. Biophys. Acta.* 1508:69–85.
40. Tsamaloukas, A., H. Szadkowska, and H. Heerklotz. 2006. Nonideal mixing in multicomponent lipid/detergent systems. *J. Phys. Condens. Matter.* In press.
41. Anderson, T. G., A. Tan, P. Ganz, and J. Seelig. 2004. Calorimetric measurement of phospholipid interaction with methyl- $\beta$ -cyclodextrin. *Biochemistry.* 43:2251–2261.
42. Huang, J. 2002. Exploration of molecular interactions in cholesterol superlattices: effect of multibody interactions. *Biophys. J.* 83: 1014–1025.
43. Cannon, B., G. Heath, J. Huang, J. A. Somerharju, J. A. Virtanen, and K. H. Cheng. 2003. Time-resolved fluorescence and Fourier transform infrared spectroscopic investigations of lateral packing defects and superlattice domains in compositionally uniform cholesterol/phosphatidylcholine bilayers. *Biophys. J.* 84:3777–3791.
44. Huang, J., and G. W. Feigenson. 1999. A microscopic model of maximum solubility of cholesterol in lipid bilayers. *Biophys. J.* 76: 2142–2157.
45. Veatch, S. L., and S. L. Keller. 2005. Seeing spots: complex phase behavior in simple membranes. *Biochim. Biophys. Acta.* 1746: 172–185.
46. Heerklotz, H., G. Lantzsch, H. Binder, and G. Klose. 1996. Thermodynamic characterization of dilute aqueous lipid/detergent mixtures of POPC and C<sub>12</sub>EO<sub>8</sub> by means of isothermal titration calorimetry. *J. Phys. Chem.* 100:6764–6774.
47. Holopainen, J. M., A. J. Metso, J.-P. Mattila, J. Arimatti, and P. K. J. Kinnunen. 2004. Evidence for the lack of a specific interaction between cholesterol and sphingomyelin. *Biophys. J.* 86:1510–1520.
48. Wang, T.-Y., R. Leventis, and J. R. Silvius. 2000. Fluorescence based evaluation of the partitioning of lipids and lipidated peptides into liquid-ordered lipid microdomains: a model for molecular partitioning into “lipid rafts”. *Biophys. J.* 79:919–933.
49. Niu, S.-L., and B. J. Litman. 2002. Manipulation of cholesterol levels in rod disk membranes by methyl- $\beta$ -cyclodextrin. *J. Biol. Chem.* 277: 20139–20145.
50. Ramstedt, B., and J. P. Slotte. 2002. Membrane properties of sphingomyelins. *FEBS Lett.* 531:33–37.